

Anatomic prior and cylindrical symmetry constraints for reconstructing susceptibility tensor

Cynthia Wisnieff^{1,2}, Tian Liu^{1,2}, and Yi Wang^{1,2}

¹Cornell University, New York City, NY, United States, ²Weill Cornell Medical College, New York City, NY, United States

Introduction: Susceptibility tensor imaging (STI) [1] is inherently prone to error propagation and requires many impractical orientations of the subject to reconstruct. Here we explore two ideas to improve the susceptibility tensor reconstruction: a) The cylindrical symmetry may be imposed on the susceptibility tensor (CSST) to improve the condition number of this problem [2]. b) The anatomic information may be used to regularize and denoise the construction of the apparent susceptibility in an orientation [3] and then apparent susceptibilities from all orientations can be used to form the anisotropic magnetic susceptibility (AMS) by Hext [4].

AMS: The apparent scalar susceptibility at the p^{th} orientation, χ_p , is estimated using the morphology enabled dipole inversion [3] from

$$\Delta B_p(\vec{k}) = \left(\frac{1}{3} - \frac{(\vec{k} \cdot \hat{B}_0)^2}{k^2} \right) FT\{\chi_p\}(\vec{k}),$$

where ΔB_p is the field shift

induced by the susceptibility tensor at each orientation p with the main magnetic field along \hat{B}_{0p} . The susceptibility tensor $\vec{\chi}$ in the subject frame is obtained by solving the set of linear equations $\hat{B}_{0p}^T \vec{\chi} \hat{B}_{0p} = \chi_p \hat{B}_{0p}^T \hat{B}_{0p}$ for all p 's.

CSST: In the tensor orthonormal frame that may be estimated in diffusion tensor imaging (DTI), the CSST is $\vec{\chi}_T = \text{diag}(\chi_{||}, \chi_{\perp}, \chi_{\perp})$. Transformation between the tensor orthonormal frame and the subject frame, R , expresses the subject frame susceptibility tensor as $\vec{\chi} = R^T \vec{\chi}_T R$.

Materials and Methods: For validation of the tensor estimation, a phantom with known susceptibility isotropy was built from Gd doped water balloons, and a phantom with known cylindrically symmetrical susceptibility anisotropy were built from a bundle of parallel carbon fibers (5). These phantoms were imaged with 12 orientations evenly distributed over a hemisphere on a 3T clinical scanner with an 8 channel head coil using a multi echo gradient echo sequence. Human data was acquired with a larger four channel bird cage head coil, a total of 13 orientations were acquired in addition to an EPI based DTI sequence. Susceptibility tensor maps were reconstructed using AMS, AMS with cylindrical symmetry (AMSCS), CSST, and STI. The anisotropy degree (AD) was computed here as, $AD = \ln(|\lambda_3|/|\lambda_1|)$, where the eigenvalues λ_i are ordered from high to low (6). For all reconstructions mean eigenvalue was fit with the known susceptibility of each balloon associated anisotropy the associated mean eigenvalues.

Results: All 4 methods generated visually similar susceptibility tensor elements and eigenvalues for both isotropic and anisotropic phantoms (Figs.1&2a), and similar ADs: -2.62 ± 0.99 for CSST, -2.35 ± 1.66 STI, -1.81 ± 0.71 AMSCS and -3.67 ± 2.18 AMS; however, the STI had more error than AMS, which had more error than CSST and AMSCS as generating artifactual ADs in the isotropic phantom (Fig.2b). Reconstructions of brain susceptibility tensor were problematic without this constraint (AMS and STI), and were more robust with cylindrical symmetry (CSST and AMSCS in Fig.3, with AMSCS seemed to be less noisy and with less AD in the globus pallidus than CSST). AD measured in the brain regions were listed in Table 1.

Discussion and Conclusion: The phantom study demonstrated the error in AD is reduced by the incorporation of anatomic prior (Fig.2b: STI vs AMS, and CSST vs AMSCS), and by the incorporation of cylindrical symmetry (Fig.2b: AMS vs AMSCS, and STI vs CSST). These improvements by constraints in reconstruction seemed to be observed in human imaging but were difficult to evaluate. Nevertheless, both CSST and AMSCS generated similar AD maps showing anisotropy in the white matter tracts.

Ref: [1] Liu,MRM:63:1411-7, 2010. [2] Wharton et. al., Proc. ISMRM:19:4515:2011. [3] Liu et. al., Neuroimage:2011. [4] Hext, Biometrika:50:1963. [5] Kimura et. al.,JAP:40:2237-40:2001. [6] Jelinek, Tectonophysics:79(3-4):T63-T67:1981.

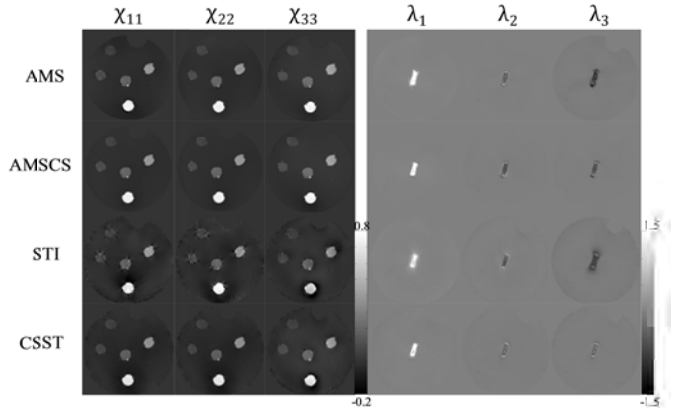


Fig. 1: Estimated Diagonal of the tensor for the isotropic phantom (left) and eigenvalues of the carbon fiber phantom (right) (ppm)

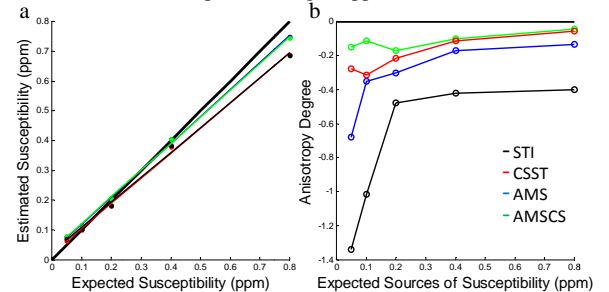


Fig. 2: Isotropic phantom, a, Mean eigenvalues and b, anisotropy of the mean

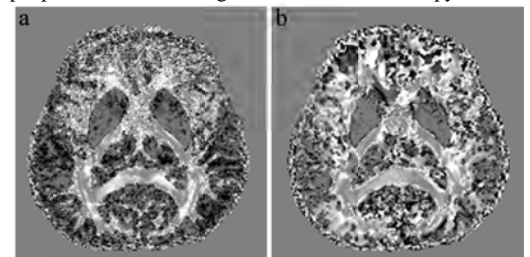


Fig. 3: AD from a) CSST and b) AMSCS

Table 1: Brain susceptibility anisotropy degree

Region	CSST	AMSCS
Globus pallidus	-0.51 ± 0.47	-0.19 ± 0.16
Corpus Callosum	1.00 ± 0.64	1.45 ± 0.64
Internal Capsule	0.87 ± 0.75	0.40 ± 0.35